Available online at www.sciencedirect.com
ScienceDirect
Journal of Hazardous Materials 148 (2007) 735–744
Journal of Hazardous Materials
www.elsevier.com/locate/jhazmat

Preparation of re-usable photocatalytic filter for degradation of Malachite Green dye under UV and vis-irradiation

F. Sayılkan [a], M. Asiltürk [b], P. Tatar [c], N. Kiraz [c], E. Arpaç [c], H. Sayılkan [a,*]

[a] *Inönü University, Faculty of Education, Department of Science, 44280 Malatya, Turkey*
[b] *Inönü University, Faculty of Arts and Science, Department of Chemistry, 44280 Malatya, Turkey*
[c] *Akdeniz University, Faculty of Arts and Science, Department of Chemistry, 07100 Antalya, Turkey*

Received 13 November 2006; received in revised form 9 March 2007; accepted 12 March 2007
Available online 15 March 2007

Abstract

Sn^{4+} doped and undoped nano-TiO_2 particles easily dispersed in water were synthesized without using organic solvent by hydrothermal process. Nanostructure-TiO_2 based thin films were prepared on flyswatter substrate, made with stainless steel, by dip-coating technique. The structure, surface and optical properties of the particles and thin films were characterized by element analysis and XRD, BET, SEM and UV/vis/NIR techniques. The photocatalytic performance of the films were tested for degradation of Malachite Green dye in solution under UV and vis-lights. The results showed that the coated flyswatter has a very high photocatalytic performance for the photodegradation of Malachite Green irradiated with UV and vis-lights. The results also proved that the hydrothermally synthesized nano-TiO_2 particles are fully anatase crystalline form and are easily dispersed in water, the coated surfaces are hydrophilic, and the doping of transition metal ion efficiently improved the degradation performance of TiO_2-coated flyswatter. The photocatalytic performances determined at both irradiation conditions were very good and were almost similar to each other for Sn^{4+} doped TiO_2-coated flyswatter and it can be repeatedly used with increasing photocatalytic activity compared to undoped TiO_2-coated flyswatter.

Keywords: Nano-TiO_2; Hydrothermal process; Sn-doping; Thin film; Photocatalysis; Malachite Green

1. Introduction

Malachite Green is one of the carcinogen organic molecules (MG), the triarylaminnethane dye, is still illegally used in aquaculture as a fungicide on larvae and juvenile fish, parasiticide and in food, textile and other industries for one or the other purposes. MG is rapidly adsorbed, metabolized to its reduced derivative leucobase leucomalachite green (LMG) and then excreted. However, it has now become a highly controversial compound due to the risks, it poses to the consumers of treated fish [1] including its effects on the immune system, reproductive system and its genotoxic and carcinogenic properties [2]. Though the use of this dye has been banned in several countries and not approved by US Food and Drug Administration [3], it is still being used in many parts of the world due to its low cost, availability and efficacy [4]. A considerable amount of research is being devoted to work out the wide spectrum of biological effects that it exerts on different animals and mankind. The US Food and Drug Administration has nominated MG as a priority chemical for carcinogenicity testing. There is concern about the fate of MG and reduced form, LMG, in aquatic and terrestrial ecosystems, since they occur as contaminants and are potential human health hazards.

The toxicity and mass production of MG, LMG or the other dyes lead to the necessity of treatment. Usually, the conventional biological treatment processes do not readily remove dyes from textile wastewater, because of their resistance to biological degradation [5,6]. Various chemical, physical and biological processes are currently used such as flocculation, ultrafiltration, adsorption, ozonation and chlorination [7]. These processes are not efficient because they appear in solid wastes, thus creating other environmental problems requiring further treatment. Therefore, it is necessary to find an effective method of wastewater treatment in order to remove hazardous dyes and organics from industry effluents [6]. One of the new methods of wastewater treatment containing dyes is their photocatalytic degradation

* Corresponding author at: Nano-TiO_2 Synthesis and Application Laboratory, Inönü University, Turkey. Tel.: +90 422 341 0010; fax: +90 422 341 0042.
E-mail address: hsayilkan@inonu.edu.tr (H. Sayılkan).

0304-3894/$ – see front matter © 2007 Elsevier B.V. All rights reserved.
doi:10.1016/j.jhazmat.2007.03.036

in solutions illuminated with UV irradiation, which contains a suitable photocatalyst. Semiconductor photocatalysis, SPC, has been the subject of extensive research over the past two decades as a possible route to providing clean water, air and surfaces [8–10]. Invariably the semiconductor is anatase titanium dioxide, because of its chemical and biological inertness, mechanical toughness, excellent photocatalytic activity, low cost and easiness of deposition [11,12]. Extensive research into SPC using TiO_2 has shown that TiO_2 photocatalyst films are self-cleaning in that most of the organic pollutants including many pesticides, surfactants, and carcinogens [13,14] that go to make up the dirt and grime that deposit on window glasses, ceramics and metal surfaces are readily mineralised by oxygen via the photocatalytic process. In addition, titania along with some other semiconductors, has the additional feature of photo-induced superhydrophilicity, PSH, in which the surface of the photocatalyst becomes much more wettable, i.e. more hydrophilic, upon irradiation with ultra-bandgap light [15,16]. As a consequence, many commercial products have emerged in recent years, including water and air purification systems and self-cleaning, antifogging and sterilizing tiles and glasses [17]. The latter in particular have met with significant commercial success and are now sold worldwide by most of the major glass manufacturers throughout the world [18,19].

When exposed to UV light, organic compounds can be broken down with TiO_2 films and enable water to spread evenly on their super hydrophilic surface to easily realize surface self-cleaning. Many researchers have focused on this subject [20,21]. In order to synthesize TiO_2, different processes have been reported, such as sol–gel process [22], non-hydrolytic sol–gel route [23], ultrasonic technique [24], chemical vapor deposition [25], microemulsion or reverse micelles and hydrothermal process [26–29]. A multitude of polar, non-polar, aqueous or organo-aqueous solvents have been used in these processes. High calcination temperature above 450 °C is usually required to form regular crystal structure in these processes, except for the hydrothermal process. However, in the meantime, the high temperature treatment can decline the surface area and surface hydroxyl or alkoxide groups on the surface of TiO_2, which provide easy dispersion in different solvent system, are lost. As far as the authors of this study are concerned there is no method employed without calcination to produce anatase TiO_2 particles, except for the hydrothermal process. Thus, the hydrothermal process was applied to synthesize mesopore Sn^{4+} doped nanosized TiO_2 particles at low temperatures without using organic solvent, which seems to be really attractive to further improve the photocatalytic activity of TiO_2. It is important to note that hydrothermally obtained powders are produced with different microstructure, morphology and phase composition by varying parameters such as temperature, pressure, duration of process, concentration of chemical species, solution concentration and pH [30–32]. Compared with the other TiO_2 powders, TiO_2 nanoparticles synthesized by hydrothermal process in this work have important advantages, such as being in anatase crystalline form, having fine particle size with more uniform distribution and high-dispersion ability either in polar or non-polar solvents and easy coating on different supporting material. In this work, photocatalytic activity of Sn-doped TiO_2 and undoped TiO_2 thin films supported on flyswatter were examined for degradation of Malachite Green (MG) in aqueous solutions under UV and vis-lights and the results were compared.

2. Experimental

2.1. Chemicals and apparatus

As starting precursors, the following reagents were employed: titanium (IV)-*n*-butoxide, [$Ti(OBu^n)_4$, 97%, Fluka], as TiO_2 source; tin(IV) chloride (Alpha, 98%) as dopant; deionized water as hydrolysis agent; 3-glycidoxypropyltrimethoxysilane (GLYMO, Aldrich, 98%) and tetraethylorthosilicate (TEOS, Aldrich, 98%) as binder reagents; hydrochloride acid (Merck, 37%) as catalyst; 2-butoxyethanol (2-BuOEtOH, Aldrich, 99%) and ethyl alcohol (EtOH, 96%) as solvents. Malachite Green (MG) which was used as a model pollutant and purchased from a local textile factory was of analytical reagent grade.

Berghoff model hydrothermal unit interfaced with a temperature (up to 240 °C) and time controller unit was used for synthesizing nano-TiO_2 photocatalysts. Phase characterization of the hydrothermally synthesized powders were studied by XRD technique. XRD patterns were recorded in the 2θ range of 10–70° with an automated X-ray diffractometer (Model D/MAX-B, Rigaku Co., Tokyo, Japan) using Cu Kα radiation ($\lambda = 1.5418$ Å) in the step scanning mode, with tube voltage of 35 kV and tube current of 30 mA. The 2θ step size was 0.04 and a scanning rate of 1.5. min^{-1} was used.

Average crystallite sizes of the nano-TiO_2 particles were also estimated from the broadening of corresponding X-ray spectral peak by Scherrer equation:

$$\beta = \left[\frac{k\lambda}{d_{hkl}\cos(\theta)}\right]$$

where λ is the wavelength of X-rays, θ the Bragg angle, d_{hkl} the average crystallite size, and β is the full width at half maximum intensity of the peak observed at $2\theta = 25.12$ (converted to radian) and k is a constant usually applied as ∼0.9.

The BET surface area, average pore diameter and micropore volume of the nanosized-TiO_2 particle was calculated from the N_2 adsorption isotherm using ASAP 2000 model BET analyzer at liquid N_2 temperature. During the BET analysis, sample was degassed at 130 °C for 4 h before N_2 adsorption. Pore size distribution of nano-TiO_2 was computed by the DFT plus method. C and H elements in the hydrothermally synthesized TiO_2 particle were analyzed by using element analyzer (LECO 932 Model). Cl was analyzed by means of potential measurement using Orion 96-17B Model Cl electrode. The amount of Sn (mol/mol, %) in Sn-doped TiO_2 was determined by AAS analysis (Perkin-Elmer, Analyst 800 model). Contact angles of the coatings with water were measured by using a goniometer (RAME HART 100-00 model). Film thickness on the stainless steel plate (2 cm × 2 cm) surface, prepared at the same coating conditions for coating of the flyswatter, was measured by Perthometer (MAHR-M1 Model).

Dye concentration in the aqueous solution after irradiation was measured by a Varian Carry 5000 model UV–vis–NIR spectrophotometer. Coated flyswatter/dye solution was irradiated with/without 400 nm cut-off filter without shaking and Solar Box 1500 model (Erichsen, Germany) radiation unit with Xe-lamp (690 W m^{-2}) and a controller for timing and power input (390–1100 W m^{-2}).

2.2. Nanosized-TiO_2 photocatalyst synthesis

TiO_2 photocatalysts were synthesized using a hydrothermal unit similar to that described by Akarsu, Arpaç and co-workers [33,34]. In a typical preparation procedure, $Ti(OBu^n)_4$ was cooled in an ice-bath, then HCl was added into cooled solution by drop using a burette. After stirring a few minutes at ambient temperature, required amount of tin(IV) chloride was suddenly added. The last solution was stirred until it formed a clear and homogeneous solution at ambient temperature. Then, the water was added into the last solution dropwise by burette. $HCl/Ti(OBu^n)_4$, $SnCl_4/Ti(OBu^n)_4$ and $H_2O/Ti(OBu^n)_4$ ratios (mol/mol) were 0.296, 0.05 and 2.06, respectively. The gelation occurred after adding water. The reaction was allowed for a few hours, then the viscose solution was obtained. The teflon crucible of 250 ml capacity was filled with sol-solution up to 80% of the total volume, then left in a pre-heated (200 °C) stainless steel autoclave device. The reaction was allowed at 200 °C for 1 h. After this time, autoclave was removed from the hydrothermal unit and cooled to room temperature, naturally. As-obtained powders were separated by decantation and dried using a rotary evaporator at 25 mbar and 40 °C for 5 h. Thus, nanosized promrise yellow TiO_2 crystallites were obtained. The undoped nano-TiO_2 with a white color particle was synthesized without using dopant with the same procedure described above.

2.3. The preparation of TiO_2 sol

The transparent TiO_2 sol prepared in water (or organic solvent) is important for preparing the high photocatalytic coating solution [33,34]. The TiO_2 particles should be included to polar groups, such as alkoxide or hydroxyl, on their surfaces for obtaining transparent TiO_2 sol in water and/or other polar solvents. It is important note that, in this case, the hydrothermal TiO_2 synthesis conditions are very important for obtaining the transparent TiO_2 sol in polar and/or non-polar solvents. The controlled hydrolysis-condensation reactions of Ti-alkoxides are realized with this process as shown below:

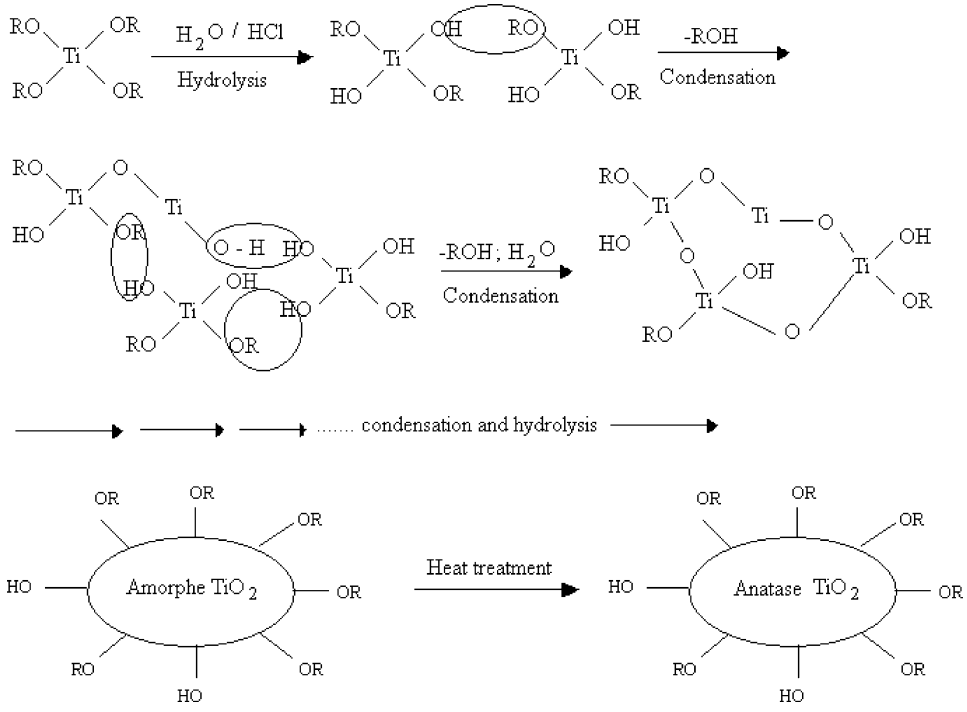

TiO_2 sol was prepared by ultrasonically dispersing the TiO_2 in deionized water without using dispersant. The water and TiO_2 particles were treatment in ultrasonic bath for a few minutes. Finally, the transparent TiO_2 sol occurred. A schematic representation of the transparent TiO_2 sol formation in polar solvent system is shown in Scheme 1.

2.4. The preparation of coating solution

The coating solution was prepared at room temperature based on the same procedure described by Arpaç and co-workers [34]. For preparing coating solution, (mol/mol ratios of each component were presented in parantheses), GLYMO was first reacted with TEOS for 10 min (GLYMO/TEOS: 1), then EtOH was added to this mixture (EtOH/GLYMO: 10.5) and stirred for 10 min. HCl was allowed to react with GLYMO/TEOS/EtOH for 10 min (HCl/GLYMO: 0.05) and finally H_2O was added to GLYMO/TEOS/EtOH/HCl and allowed to react for 10 min (H_2O/GLYMO: 6.3). Thus, the coating solution was prepared. TiO_2 sol (10 g) was added into the

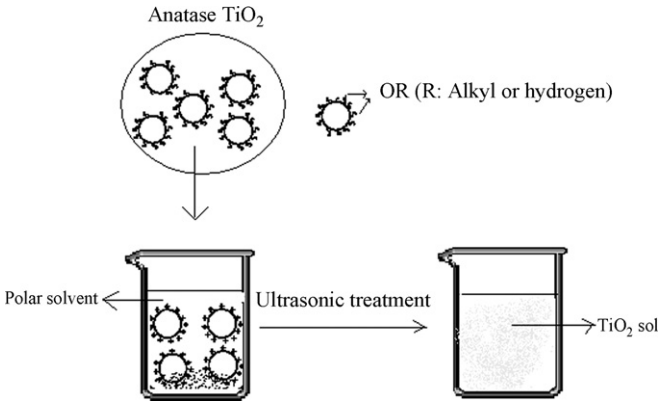

Scheme 1. Transparent TiO_2 sol formation in polar solvent system.

coating solution (10 g) and the mixture was stirred for 15 min before adding 2-BuOEtOH (8 g) stirring for 40 h. Finally, transparent and colorless solution was obtained. Two sides of the flyswatter, which has pores with 0.2 cm × 0.2 cm, surfaces were coated with this solution using dip-coating technique (drawing and dipping rate are 3.2 cm/min), and the pores of the flyswatter was opened by using an air blower. Since it is necessary to filter the water either in industrial applications or in swimming pools before the remediation or the removal of contaminants and provided this type of filters can remediate or clean the contaminants directly by catalytic effect, an important difficulty will be in situ eliminated, flyswatter gained photocatalytic activity was found applicable and used in this study.

For curing, the coated surface was treated at 100 °C for 60 min. For obtaining hydrophilic surface, the coated surfaces were irradiated under UV lamp operating at 8 W for 60 min. The amount of TiO_2 in coatings prepared doped and undoped TiO_2 was 52.63 wt%, as calculated by taking consideration the amount of SiO_2 originating from GLYMO and TEOS and TiO_2 from TiO_2 sol.

2.5. Photocatalytic degradation of Malachite Green

Malachite Green (MG) is a common chemical that is used extensively in a variety of industrial applications. Therefore, it is chosen to be as a model pollutant. The photocatalytic degradation intermediates of MG were not determined in this study. The coated flyswatter (2.5 cm × 5 cm) was immersed into 25 ml aqueous MG solution with a concentration of 5 mg/l in a polystyrene reaction cell, which has six separate sample compartments and one cover. The cell was immediately located in the Solar Box ready for UV-irradiation inducing the photochemical reaction to proceed. The coated flyswatter/dye solution was irradiated in the vertical direction without shaking and the distance between the UV lamp and flyswatter/dye solution system was kept within 20 cm. The change of MG concentration with respect to irradiation time was measured using a UV/vis/NIR spectrophotometer. The photocatalytic performance of the coated flyswatter was determined without cut-off filter for UV irradiation, and with 400 nm cut-off filter for vis irradiation. The photocatalytic reactor system used for testing the photocatalytic performance of undoped and Sn doped TiO_2-coated surfaces is shown in Scheme 2.

2.6. Catalyst re-use studies

Flyswatters coated with undoped and Sn-doped TiO_2 were repetitively used to degrade MG under UV and vis-lights. After the first use, so-used flyswatter was again employed to degrade a fresh MG solution under the same conditions. The process was repeated for three times. Before using repeatedly, the coated

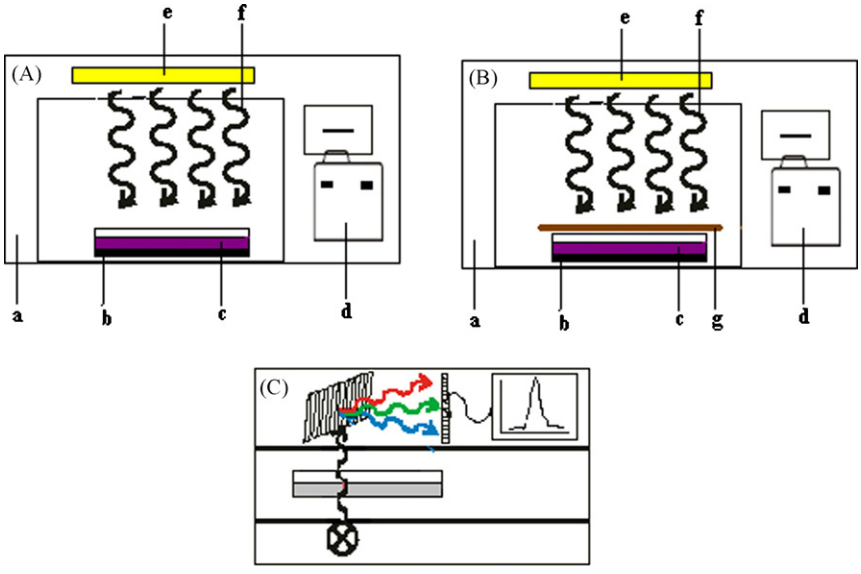

Scheme 2. Photoreactor system. (A) UV irradiation applied without filter, (B) vis irradiation applied with UV cut-off filter, (C) UV measurement after irradiation. ((a) Solar Box irradiation unit, (b) Sn doped TiO_2-coated glass plate, (c) dye solution, (d) control unit of the Solar Box, (e) UV lamp, (f) UV lights and (g) glass UV filter).

flyswatters was stored in the dark at room temperature for a night.

3. Results and discussion

The XRD of hydrothermally synthesized TiO_2 samples, as presented in Fig. 1, indicates that the TiO_2 particles in the anatase crystalline form corresponds well with the PDF#21-1272 data files. It was found that all peaks were observed at 25.16°, 37.91°, 48.19°, 55.01° (for undoped TiO_2) and 25.12°, 37.88°, 48.07° and 54.52° (for Sn-doped TiO_2). 2θ values are consistent with anatase (1 0 1), (0 0 4), (2 0 0) and (2 1 1) spacing. The other crystalline forms of TiO_2, i.e. rutile and brookite, have not been detected, as reported in our previous works [34]. The present and previous works show that Sn-doped and undoped TiO_2 photocatalysts which have same crystallite structure can be synthesized by the different crystallization routes from different precursor [33,34]. In addition, no Sn phase, as examined according to the sensitivity of XRD method, was found in XRD pattern. Based on the main chemical state of Sn^{4+}, it can be concluded that Sn ions completely dissolved among the anatase crystallite in the studied composition [35]. In the region of 10–70°, the shape of diffractive peaks of the crystal planes of Sn-doped TiO_2 (curve b) is almost similar to that of undoped TiO_2 (curve a), however the position of the diffraction peaks between of Sn-doped TiO_2 and undoped TiO_2 are slightly shifts to smaller diffraction angles. It is known that there are two kinds of doping modes; interstitial and substitutional, for doped metal ions in oxides, depending primarily on the electronegativity and ionic radius of the doping metal ions. If the electronegativity and ionic radius of the doping metal ions match those of the lattice metal ion in oxides, the doping metal ion will substitute itself for the lattice in the doping reactive process (substitutional mode). If the electronegativity of the doping metal ion approaches that of the lattice metal ion and its ionic radius is smaller than that of the lattice metal ion, the oxide lattice spacing will be larger than the ionic radius of the lattice metal ions, which will enter into the crystal cell of the oxide (interstitial mode) [21,36]. Since the electronegativity and the ionic radius of Sn^{4+} ion (1.8, 69 pm) approach those of Ti^{4+} ion (1.5, 53 pm) in TiO_2 [24], it is expected that Sn^{4+} ions will replace lattice Ti^{4+} ions and thus occupy lattice Ti^{4+} positions in the doping reactive process. The ionic radius of the doping Sn^{4+} ion is larger than that of the lattice and increment the lattice

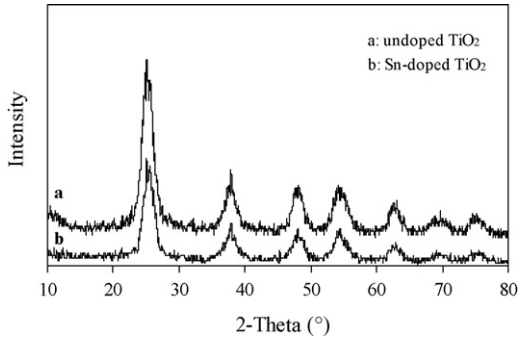

Fig. 1. XRD patterns of nano-TiO_2 particles.

Table 1
Some physicochemical characteristics of the synthesized undoped and Sn-doped TiO_2 and the films

	Undoped $^{16}TiO_2$	Sn-doped TiO_2
Particle property		
Crystalline type	Anatase	Anatase
Crystallite size (nm)	9.96	9.24
BET surface area ($m^2\ g^{-1}$)	40.84	97.83
Micropore area ($m^2\ g^{-1}$)	39.31	19.87
Micropore volume ($cm^3\ g^{-1}$)	0.022	0.011
Adsorption average pore diameter (Å)	13.12	21.16
Film property		
Film thickness (μm)[a]	15	21
Contact angles with water (before/after irradiation)[a]	60°/25°	69°/8°

[a] These measurements were performed for the coated stainless steel plate (5 cm × 5 cm).

parameters and cell volume of Sn-doped TiO_2 compared with those of TiO_2. As a result, the position of all the diffraction peaks of Sn-doped TiO_2 should slightly lower diffraction angles.

According to Sn analysis carried out by AAS in the centrifuged solution obtained after the hydrothermal treatment, the doping ratio was obtained as 4.92 [Sn^{4+}/$Ti(OBu^n)_4$; mol/mol, %]. This result shows that, the Sn^{4+} ions was almost doped into TiO_2 lattice. The other elements (C, H and Cl) in undoped TiO_2 particle were 10.49% C, 2.52% H and 2.90% Cl, which means that purity of the undoped TiO_2 is 84.09%, and in Sn doped TiO_2 particle were 10.05% C, 2.57% H and 2.97% Cl, which means that purity of the Sn-doped TiO_2 is 82.18%.

Some of the physicochemical properties of the synthesized Sn doped and undoped TiO_2 particles and the films are shown in Table 1.

As can be seen from the table, while the BET surface area and adsorption average pore diameter of the undoped TiO_2 are smaller, micropore area, crystallite size and micropore volume are bigger than Sn doped TiO_2. From these properties, especially surface area affects the photocatalytic properties of these photocatalysts. According to the result of DFT plus method [37], microporosity (percentage of micropore to total pore volume, V_{mi}/V_{tot}) dominated and distributed very little in the range of 14–20 Å for undoped TiO_2. Whereas, mesoporosity (percentage of mesopore to total pore volume, V_{ms}/V_{tot}) dominated and distributed large area in the range of 12–32 Å for Sn-doped TiO_2. Total pore volume was estimated from nitrogen adsorption at a relative pressure of 0.995. The microporosity and the mesoporosity were 98.6% and 1.4%, respectively, for undoped TiO_2. The mesoporosity and microporosity for Sn-doped TiO_2 were 79% and 21%, respectively. On the other hand, the TiO_2 particles have just a little bit macroporosity in the 50.5–100.5 Å as less than 0.1%.

UV/vis absorption spectra of TiO_2 particles synthesized in this work are identical to the spectra reported in a previous work [34]. The doping Sn^{4+} results in a sharp increase in the absorption of TiO_2 photocatalyst in visible region, leaving unaffected intrinsic band gap of anatase TiO_2. The band edge absorption at <380 nm is accompanied by a broad and continuously decreas-

ing absorption in the range 380–560 nm. The greatly red-shift (380–560 nm) can be attributed to the electron transfer transitions between conduction band (CB) and/or valance band (VB) of SnO_2 and conduction band (CB) and/or valance band (VB) of TiO_2. The extended absorbance of Sn doped TiO_2 photocatalyst in the visible region provides a possibility for enhancing the photocatalytic performance of TiO_2.

While SnO_2 and TiO_2 are quite similar in spectral responses as both are large bandgap semiconductors, SnO_2 has a wide band gap energy than TiO_2 (E_g, bandgap energy, for SnO_2 = 3.8 eV while E_g for TiO_2 = 3.2 eV) [38]. Though the band gap of SnO_2 is wider than that of TiO_2, its conduction band is at a lower energy level than that of TiO_2 as shown in Scheme 2. The electrical conductivity of SnO_2 is better than that of TiO_2. Hence, in a mixture of TiO_2 and SnO_2, it could be expected that the photogenerated electrons from TiO_2 is transferred easily into the SnO_2 underlayer, $[(TiO_2)e^-_{CB} \rightarrow (SnO_2)e^-_{CB}]$, and holes oppositely flow into the TiO_2 overlayer, $[(SnO_2)h^+_{VB} \rightarrow (TiO_2)h^+_{VB}]$ [39,40]. Consequently, more holes reach the TiO_2 surface to oxidation thereat in surface. The electrons would be accumulated in the SnO_2 underlayer. In addition, as the molar ratio of SnO_2 is lower than that of TiO_2, each SnO_2 particle is surrounded more by TiO_2 particles, the photogenerated electron from TiO_2 conduction band may be passed to the SnO_2 conduction band or the electrons from the SnO_2 valence band may be excited to its conduction band by illumination. However, since SnO_2 particle is surrounded by many TiO_2, to which it cannot transfer the photogenerated electron, the electrons cannot further travel to the outer circuit and so on. It can be concluded that this phenomenon plays important role in the photocatalytic performances of these type of semiconductors.

Typical SEM images of Sn-doped and undoped TiO_2 particles are shown in Fig. 2. Fig. 2a and b indicates that shape of the particles are quite similar to each other and likely to become spherical in general. In the SEM images seen that the some TiO_2 particles are agglomerates. The agglomeration may result from the hydrothermal treatment conditions. However the size distribution of the powder was not determined, the size of the particles varies in the range of 1.02–8.25 μm for Sn-doped TiO_2 and of 1.07–11.72 μm for undoped TiO_2, as measured using the SEM images. Introduction of Sn^{4+} ion decreased the size of the powder and gained more spherical shapes.

One interesting result obtained in this work is that the crystallite size and the particle size (Table 1 and Fig. 2) of the Sn^{4+} doped TiO_2 were smaller than that of undoped TiO_2, which can signify that the presence of Sn^{4+} in the reactional media might

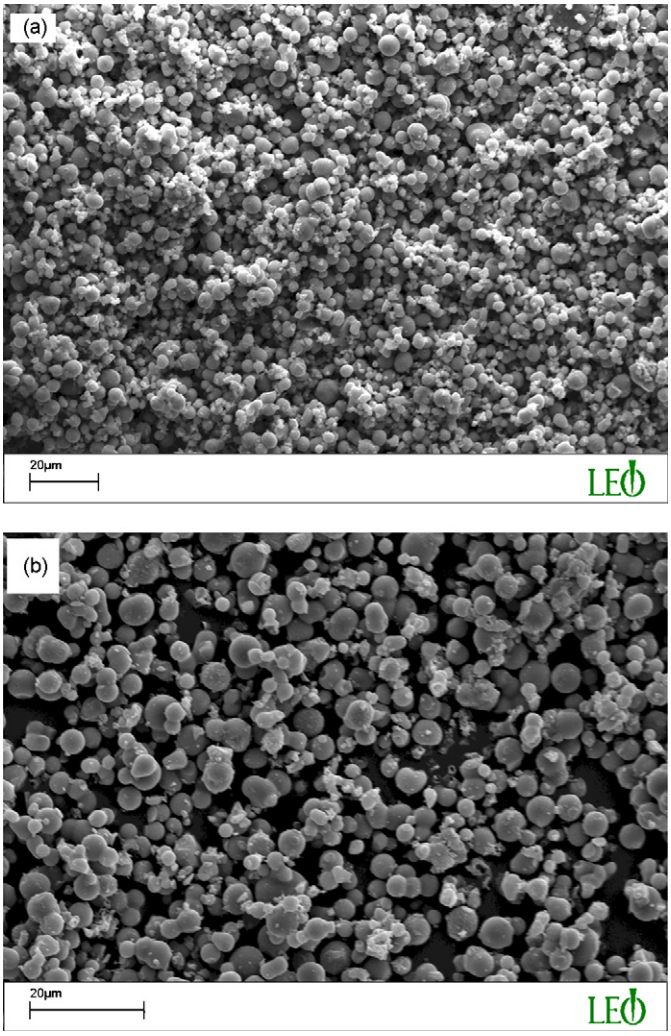

Fig. 2. Typical SEM microphotograph of: (a) undoped TiO_2 particle and (b) Sn-doped TiO_2 particle.

be used to control the particle and crystallite sizes of the oxides. Oliviera et al. [41] reported that the particle size of $(Ti,Sn)O_2$ mixed oxides prepared by the sol–gel process lower than the pure TiO_2. Leite et al. [42] also reported a novel approach to control particle size of Nb_2O_5 doped (5 mol%) SnO_2 prepared by the polymeric precursors method. They observed that Nb_2O_5–SnO_2 mixed oxide is formed with lower crystallite size than the pure SnO_2, with an Nb_2O_5–SnO_2 solid solution restricted to the surface of particles. The lower crystallite size of doped particles was attributed to this surface effect, with the Nb_2O_5 preventing

Table 2
Identification of the *N*-de-methylation intermediates of the MG dye by HPLC–ESI–MS

N-de-methylation intermediates	ESI–MS peaks (*m*/*z*)	Absorption maximum (nm)
Bis(*p*-dimethylaminophenyl)phenylmethylium	329.26	620.1
(*p*-Dimethylaminophenyl)(*p*-methylaminophenyl)phenylmethylium	315.18	607.9
(*p*-Methylaminophenyl)(*p*-methylaminophenyl)phenylmethylium	301.22	598.1
(*p*-Dimethylaminophenyl)(*p*-aminophenyl)phenylmethylium	301.22	599.0
(*p*-Methylaminophenyl)(*p*-aminophenyl)phenylmethylium	287.08	589.6
Bis(*p*-aminophenyl)phenylmethylium	NA	NA

the formation of necks between particles and the process of coalescence. The similar effect can be occurring in Sn^{4+} doped TiO_2 particle synthesized in our work. There are important differences between the oxide of this present study and their oxides. For example, Sn^{4+} doped and undoped TiO_2 particles were synthesized by the hydrothermal process at low temperature (200 °C) and very low reaction time (1 h), organic solvent is not used during the synthesis reaction, the obtained particles were fully anatase crystalline form and easily dispersed in water without using dispersant.

As can be also seen from Table 1, the film thickness was measured as 15 and 21 μm for Sn^{4+} doped and undoped TiO_2-coated surfaces, respectively. In addition, the contact angles of the irradiated surfaces with water were found to be 8° and 25° for Sn^{4+} doped and undoped TiO_2 (not shown here)-coated stainless steel plate surfaces. These results reveal that the contact angle decreases during the irradiation. For example, while the contact angle was 8° and 25° on the irradiated surfaces, they were 60° and 69° on the unirradiated surface. The decrease in the contact angle can be attributed to the reaction of produced electrons and holes in a different way. According to Fujishima et al. [20], the electrons tend to reduce the Ti(IV) cations to the Ti(III) state and the holes oxidize the O^{2-} anions. In this process oxygen atoms are rejected, creating oxygen vacancies. Water molecules can then occupy these oxygen vacancies, producing adsorbed OH groups, which tend to make the surface hydrophilic. Therefore, we can conclude that the irradiated surface has hydrophilic property. This property has an important role for photocatalytic properties. As can be seen from Fig. 3, water drop spreads as a thin film on the irradiated stainless steel plate surfaces coated with Sn^{4+} doped TiO_2.

The photocatalytic activity results for Sn-doped and undoped TiO_2-coated flyswatters exposed for the photodegradation of MG under both UV and vis-lights are shown in Fig. 4a–d.

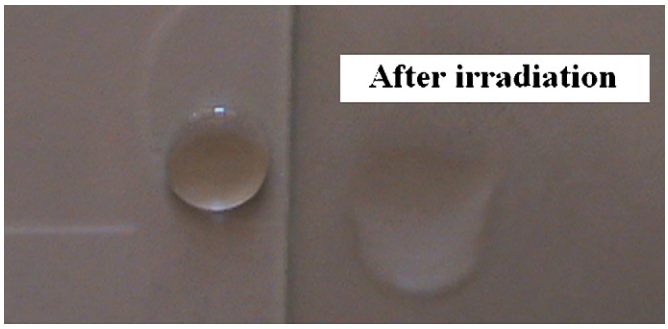

Fig. 3. Hydrophilic surface image on the stainless steel plate.

As shown in Fig. 4, the photocatalytic performance of Sn-doped TiO_2 film for the degradation of MG is higher than that of the undoped TiO_2 thin film under UV and vis-lights. According to results of repeated usage experiments performed under UV and vis-lights, doping of Sn^{4+} ion improves the photocatalytic activity. After the third use, the photocatalytic performance of Sn-doped TiO_2 thin film was almost similar to first, second and third use under UV and vis-lights (Fig. 4a and b), whereas the undoped-TiO_2 thin film showed a decreased photocatalytic activity from first to third use (Fig. 4c and d). After irradiation for 130 min, the MG (5 mg/l) was degraded as 96%, 94% and 93% after first, second and third use under UV irradiation, and was degraded as 94%, 94% and 93% under vis irradiation, respectively, with Sn^{4+} doped TiO_2 thin film. On the other hand, the MG was degraded as 89%, 87% and 84% after first, second and third use under UV irradiation, and was degraded as 74%, 68% and 62% under vis irradiation with undoped TiO_2 thin film, respectively. It is known that the photocatalytic activity of anatase TiO_2 is very high under UV irradiation. Doping of Sn^{4+} ion also improves the photocatalytic activity of flyswatter more evidently under both UV and vis irradiation. In our previous work, the undoped TiO_2-coated glass surface showed a decreased the pho-

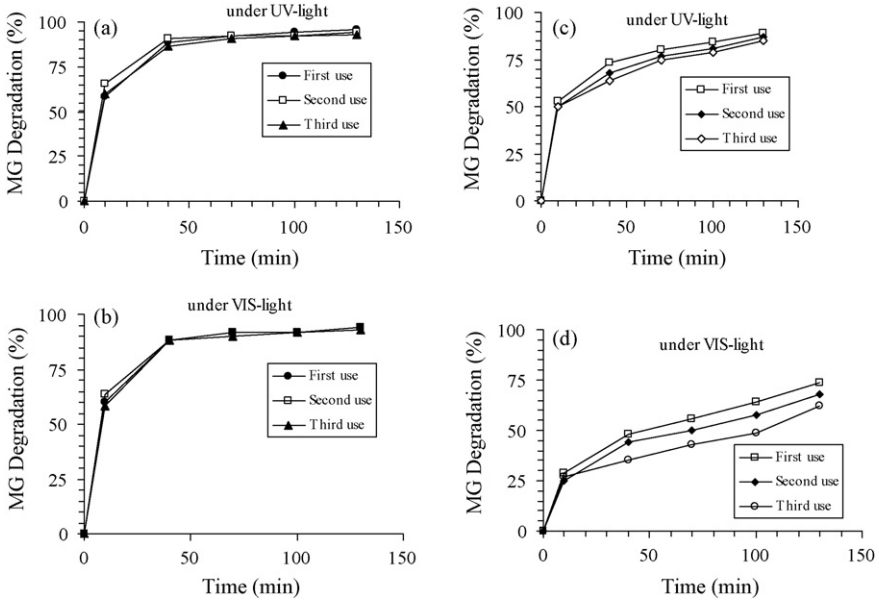

Fig. 4. Photodegradation of MG with Sn^{4+} doped (a and b) and undoped TiO_2 (c and d) coated surfaces under UV (a and c) and vis-lights (b and d).

tocatalytic performance from first to third or second use under UV and vis irradiation [34]. According to the results of repeated usage experiments performed under both irradiation conditions, the Sn^{4+} doped TiO_2-coated surface showed higher photocatalytic performance than undoped TiO_2-coated surface and its photocatalytic performance almost similar each other under UV and vis-lights from first to third use. In this study, degradation products of MG were not characterized. Nevertheless, a variety of studies where either commercial Degussa P-25 TiO_2 or sol–gel synthesized TiO_2 was used as catalyst endeavored to establish the degradation end-products. Some researchers have reported that, most oxidative *N*-de-alkylation processes are preceded by the formation of a nitrogen centered radical [43–45], but the destruction of the dye chromophore structures is preceded by the generation of a carbon-centered radical [46–48] According to this statement, the degradation of MG must occur via two different photooxidation pathways (destruction of the chromophore structure and *N*-de-methylation) due to the formation of the different radicals (either carbon-centered or nitrogen centered radicals). There is no doubt that electron injection from the dye to the positive holes of TiO_2 yields the dye cationic radical (Dye^+). After this stage, Dye^+ can undergo hydrolysis and/or deprotonation pathways of the dye cationic radicals, which in turn are determined by the different adsorption modes of MG on the particles surface [49]. When the MG dye molecules are located near the TiO_2 surface due to the dimethylamine group, the *N*-de-methylation process predominates during the initial stages. Destruction of the chromophore ring structure occurs mostly only after full *N*-de-methylation of the dye occurs. As Chen et al. [50] have reported, end-products arising until the MG reaches total mineralization, which were determined by HPLC–ESI–MS are listed in Table 2. The same results were obtained by the other works [51,52]. Accordingly, the degradation of MG dye in solution containing Sn^{4+} doped or undoped TiO_2 under UV and vis-lights is expected to occur by means of *N*-de-methylation.

There are various reasons for the increase photocatalytic performance:

(a) High photocatalytic activity of Sn-doped TiO_2 film may be related to high surface area of the nano-Sn^{4+} doped TiO_2 particles as well as their mesoporous structure. It is well known that, as the particle size decreases, the surface area increases, and as the process is adsorption dependent, the photocatalytic degradation rate also increases. Thus, Sn^{4+}-doped TiO_2-coated surface, which has a surface area of $97.83\,m^2\,g^{-1}$, showed that higher photocatalytic performance than undoped-TiO_2, which has a surface area of $40.84\,m^2\,g^{-1}$. Dagan and Tomkiewicz [53] and Tomkiewicz et al. [54] also showed that TiO_2 with a surface area of $600\,m^2\,g^{-1}$ showed greater activity than commercial Degussa P-25 which has a surface area of $55\,m^2\,g^{-1}$.

(b) Dopant Sn^{4+} improves electron transfer efficiency from the LUMO band of MG to the conduction band of Sn-doped TiO_2, subsequently increasing the amount of radicals as shown in Scheme 3.

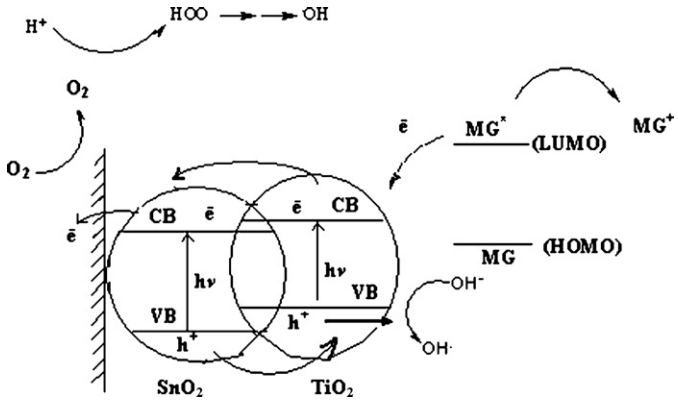

Scheme 3. Schematic representation of electron transfer from MG (LUMO) to TiO_2 (CB).

(c) It has been presumed that the high photocatalytic performance can be ascribed to the Sn ions located in the TiO_2 lattice. In this case, some of the lattice Ti in TiO_2 is substituted by Sn^{4+} ions, the cell volume increases and lattice distortion and deformation are induced. This will result in the formation of more surface defects including coordinatively unsaturated surface cations such as Ti^{4+} and Sn^{4+} on the film surface. During the photocatalytic reaction, dye molecules can be captured by the surface defects on the Sn-doped TiO_2 film and are immediately oxidized by photogenerated holes from the valence band of the catalyst [55]. At the same time, these surface defects can efficiently capture O_2 molecules to form O_2^- active species for further photocatalytic degradation of dye molecules. The photogenerated electrons on the conduction band of TiO_2 must experience energy leaping over a potential barrier to reach the surface and be captured by the surface adsorbed O_2 molecules. At the same time, accumulated photogenerated electrons at the bottom of the bent conduction band [$(SnO_2)e^-_{CB}$] will increase the probability of electron–hole recombination during the photocatalytic reaction. After Sn-doping, since the conduction band energy level of SnO_2 is lower than that of TiO_2, photogenerated electrons on the particle surface generated by visible light at the conduction band of SnO_2 can be captured directly by the efficiently adsorbed O_2 molecules on the Sn doped TiO_2 surface. In case of UV light, the photogenerated electrons at the conduction band can be transferred to the conduction band of SnO_2 and can then be captured by adsorbed O_2 molecules on the Sn doped TiO_2 surface. This will accelerate the separation of the holes and electrons, prohibiting their recombination. As a result, more photogenerated electrons and holes contribute to the photocatalytic reaction, improving the photocatalytic performance activities under both UV and vis-lights. Moreover, Sn ions might be in the substitution sites of Ti, forming a solid-state compound like $Ti_{1-x}Sn_xO_2$, [56]. $Ti_{1-x}Sn_xO_2$ may have a high photocatalytic performance causing a high tendency to degrade the MG. Besides, the Sn-doped TiO_2 particle has strong UV-light absorption ability, denoting that it can effectively be utilized for photocatalytic applications under vis-irradiation. At the same time, it is seen that the Sn-

doped TiO_2 particle has strong UV-light absorption ability. This also denotes that the Sn-doped TiO_2 particle can effectively be utilized under vis-irradiation for photocatalytic applications.

(d) All the nano-TiO_2 particles in coating can be transferred onto the Sn-doped TiO_2-coated surface during the irradiation resulting in a high photocatalytic performance.

(e) The high photocatalytic performance of the coated plate can also be related to its surface, which has hydrophilic property.

These reasons (d and e) are consistent with the results obtained by Schmidt et al. [57].

4. Conclusion

Nano-sized Sn-doped and undoped TiO_2 particles were synthesized by hydrothermal process at low temperature and very transparent and smooth thin films on flyswatter substrate, made with stainless steel, were prepared by dip-coating technique. It was found that the synthesized nano-TiO_2-coated surfaces have hydrophilic property. These particles synthesised in our work have much advantages than that the TiO_2 particles synthesised by the other process, for example, these particles were synthesised without using organic solvent such as alcohols, they were fully anatase crystal form, easily dispersed in polar and/or apolar solvent system (amphiphilic property) and they can be easily used to obtained of thin or thick film on different surfaces. Doping of the Sn^{4+} ion decreases the particle size but it increases the surface area. The photocatalytic performance of Sn-doped TiO_2 thin film for the photodegradation of MG is very high than the uncoated surface both under UV and vis-lights. Active sites on the coated surface are increased since the flyswatter has a high surface are, hence, the photodegradation performance of the catalyst increased. It can be suggested that, this coated surfaces prepared in our experiments can be used for cleaning of the pool water, deodorizing the interior of room air and preparing self-cleaning and/or antibacterial surfaces.

Acknowledgement

The authors gratefully acknowledge the financial support of T.R. Prime Ministry State Planning Organization (Project number: 2005 DPT.120.150).

References

[1] D.J. Alderman, R.S. Clifton-Hadley, J. Fish Dis. 16 (4) (1993) 297.
[2] K.V.K. Rao, Toxicol. Lett. 81 (2–3) (1995) 107.
[3] C.F. Chang, C.H. Yang, Y.O. Shu, Asian Fish Soc. (2001) P31–P39.
[4] R.A. Schnick, Prog. Fish Cult. 50 (1988) 190.
[5] T. Sauer, G.C. Neto, H.J. José, R.F.P.M. Moreira, J. Photochem. Photobiol. A: Chem. 149 (2002) 147.
[6] N. Daneshvar, D. Salari, D.A.R. Khataee, Photochem. Photobiol. A: Chem. 157 (2003) 111.
[7] K.R. Ramakrishna, T. Viraraghavan, Water Sci. Technol. 36 (2) (1997) 189.
[8] A. Kumbhar, G. Chumanov, J. Nanopart. Res. 7 (2005) 489.
[9] W.Y. Zhou, S.Q. Tang, L. Wan, K. Wei, D.Y. Li, J. Mater. Sci. 39 (2004) 1139.
[10] S.J. Hwang, C. Petucci, D. Raftery, J. Am. Chem. Soc. 120 (1998) 4388.
[11] M. Andersson, L. Österlund, S. Ljungström, A. Palmqvist, J. Phys. Chem. B 106 (41) (2002) 10674.
[12] H. Tada, A. Hattori, Y. Tokihisa, K. Imai, N. Tohge, S. Ito, J. Phys. Chem. B 104 (19) (2000) 4585.
[13] A. Mills, S. LeHunte, J. Photochem. Photobiol. A: Chem. 108 (1997) 1.
[14] M.R. Hoffmann, S.T. Martin, W. Choi, D.W. Bahnemann, Chem. Rev. 95 (1995) 69.
[15] A. Fujishima, R. Wang, K. Hashimoto, T. Watanabe, M. Chikuni, E. Kojima, A. Kitamura, M. Shimohigoshi, Adv. Mater. 10 (1998) 135.
[16] A. Fujishima, T.N. Rao, D. Tryk, J. Photochem. Photobiol. C: Photochem. Rev. 1 (2000) 1.
[17] A. Mills, S.K. Lee, J. Photochem. Photobiol. A: Chem. 152 (2002) 233, and references therein.
[18] M. Reisch, Chem. Eng. News 79 (2001) 8.
[19] K.D. Sanderson, A. Mills, S. Hurst, A. Lepre, T. McKittrick, D. Rimmer, L. Ye, SVC 46th Annual Technical Conference Proceedings, Society of Vacuum Coaters, Albuquerque, NM, 2003, p. 203.
[20] A. Fujishima, T.N. Rao, D.A. Tryk, J. Photochem. Photobiol. C 1 (2000) 1.
[21] L. Zhang, Y. Zhu, Y. He, W. Li, H. Sun, Appl. Catal. B: Environ. 40 (2003) 287.
[22] Y. Cao, W. Yang, W. Zhang, G. Liu, P. Yue, New. J. Chem. 28 (2004) 218.
[23] M. Bockmeyer, P. Lobmann, Chem. Mater. 18 (18) (2006) 4478.
[24] V. Lafond, P.H. Mutin, A. Vioux, J. Mol. Catal. A: Chem. 182/183 (2002) 81.
[25] Z. Ding, X. Hu, G.O. Lu, P.-L. Yue, P.F. Greenfield, Langmuir 16 (15) (2000) 6216.
[26] E. Hosono, S. Fujihara, K. Kakiuchi, H. Imai, J. Am. Chem. Soc. 126 (25) (2004) 7790.
[27] S. Jeon, P.V. Braun, Chem. Mater. 15 (6) (2003) 1256.
[28] H.Z. Zhang, M. Finnegan, J.F. Banfield, Nano Lett. 1 (2001) 81.
[29] X.S. Ju, P. Huang, N. Xu, J. Shi, J. Membr. Sci. 202 (2002) 63.
[30] K. Byrappa, M. Yoshimura, Handbook of Hydrothermal Technology, William Andrew Publishing, USA, New York, 2001, p. 875.
[31] G. Demazeau, J. Mater. Chem. 9 (1999) 15.
[32] G. Demazeau, Proceedings of the Joint Sixth International Symposium on Hydrothermal Reactions and Fourth Conference on Solvo-Thermal Reactions, Kochi, Japan, July 25–28, 2000, p. 1.
[33] M. Akarsu, M. Asilturk, F. Sayılkan, N. Kiraz, E. Arpaç, H. Sayılkan, Turk. J. Chem. 30 (3) (2006) 333.
[34] M. Asiltürk, F. Sayılkan, S. Erdemoglu, M. Akarsu, H. Sayılkan, M. Erdemoglu, E. Arpaç, J. Hazard. Mater. 129 (1–3) (2006) 164.
[35] S. Mahanty, S. Roy, S. Sen, J. Cryst. Growth 261 (2004) 77.
[36] Y.L. Xu, The Basics of Semiconducting Oxides and Compounds, Press of Xi'an Electronic Science and Technology University, Xi'an, 1991.
[37] J.P. Olivier, J. Porous Mater. 2 (1995) 9.
[38] K. Vinodgopal, P.V. Kamat, Environ. Sci. Technol. 29 (1995) 841.
[39] R. Subasri, T. Shinohara, Electrochem. Commun. 5 (2003) 897.
[40] A. Hattori, Y. Tokihisa, H. Tada, N. Tohge, S. Ito, J. Sol–Gel Sci. Technol. 22 (2001) 53.
[41] M.M. Oliveira, D.C. Schnitter, A.J.G. Zarbin, Chem. Mater. 15 (20031903).
[42] E.R. Leite, I.T. Weber, E. Longo, J.A. Varela, Adv. Mater. 12 (2000) 965.
[43] G. Galliani, B. Rindone, C. Scolastico, Tetrahedron Lett. (1975) 1285.
[44] F.C. Shaefer, W.D. Zimmermann, J. Org. Chem. 35 (1970) 1970.
[45] B.L. Laube, M.R. Asirvatham, C.K. Mann, J. Org. Chem. 42 (1977) 670.
[46] H. Kyung, J. Lee, W. Choi, Environ. Sci. Technol. 39 (2005) 2376.
[47] G. Liu, T. Wu, J. Zhao, K. Wu, K. Oikawa, H. Hidaka, N. Serpone, New J. Chem. 24 (2000) 411.
[48] G. Liu, J. Zhao, K. Wu, K. Oikawa, H. Hidaka, N. Serpone, Environ. Sci. Technol. 33 (1999) 2081.
[49] G. Liu, X. Li, J. Zhao, H. Hidaka, N. Serpone, Environ. Sci. Technol. 34 (2000) 3982.

[50] C.C. Chen, C.S. Lu, Y.C. Chung, J.L. Jan, J. Hazard. Mater. 141 (2007) 520.
[51] Y. Bessekhouad, D. Robert, J.C. Weber, J. Photochem. Photobiol. A: Chem. 157 (1) (2003) 47.
[52] J. Zhao, K. Wu, T. Wu, H. Hidaka, N. Serpone, J. Chem. Soc., Faraday Trans. 94 (1998) 673.
[53] G. Dagan, M. Tomkiewicz, J. Phys. Chem. 97 (1993) 12651.
[54] M. Tomkiewicz, G. Dagan, Z. Zhu, Res. Chem. Intermed. 20 (1994) 701.
[55] J.C. Yu, J. Lin, R.V.M. Kwok, J. Phys. Chem. B. 102 (1998) 5094.
[56] F. Fresno, C. Guillard, J.M. Coronado, J.M. Chovelon, D. Tudela, J. Soria, J.M. Herrmann, J. Photochem. Photobiol. A: Chem. 173 (2005) 13.
[57] H. Schmidt, M. Akarsu, T.S. Muller, K. Moh, G. Schafer, D.J. Strauss, M. Naumann, Res. Chem. Intermed. 31 (4–6) (2005) 535.